



Removal of copper from aqueous solution using alluvial soil of Indian origin: Equilibrium, Kinetic and Thermodynamic study

B. Das, N.K. Mondal*, R. Bhaumik, P. Roy, K.C. Pal, C.R. Das

Department of Environmental Science, The University of Burdwan, Burdwan-713104, India.

Received 16 June 2012, Revised 3 Mar 2013, Accepted 3 Mar 2013

* Corresponding author: E-mail: nkmenvbu@gmail.com, Tel : +919434545694

Abstract

In the present study adsorption of copper (II) ions from aqueous solution by alluvial soil of Bhagirathi River was investigated under batch mode. The influence of solution pH, sorbent dose, copper concentration, contact time, stirring rate and temperature was studied. The copper adsorption was favored with maximum adsorption at pH 6.0. Sorption equilibrium time was observed in 60 min. The equilibrium adsorption data were correlated with Freundlich, Langmuir, Dubinin-Radushkevich, Temkin and BET adsorption isotherm models. The kinetics of the adsorption process was tested by pseudo-first-order, pseudo-second order, Elovich, Intra-particle diffusion and surface mass transfer models. It was shown that adsorption of copper could be described by the pseudo-second order kinetic model. The activation energy of the adsorption process (E_a) was found to be -17.63 kJ/mol by using the Arrhenius equation, indicating physisorption nature of copper (II) adsorption onto adsorbent. Thermodynamic parameters such as Gibbs free energy (ΔG°), the enthalpy (ΔH°) and the entropy change of sorption (ΔS°) have also been evaluated and it has been found that the adsorption process was spontaneous, feasible and exothermic in nature. The results indicated that alluvial soil of Bhagirathi River can be used as an effective and low-cost adsorbent to remove copper (II) from aqueous solution.

Keywords: Copper (II) ions, activation energy, Langmuir, surface mass transfer

1. Introduction

Copper is one of the toxic heavy metal that is largely released into the environment from various types of industries such as electronics, metal plating, automotive, battery, etc. As a trace element, copper is essential to maintain human body metabolism. However, excessive intake of copper can cause serious health problems such as damage to heart, kidney, liver, pancreas, brain, intestinal distress and anemia [1]. The World Health Organization (WHO) recommended a maximum acceptable concentration of Cu (II) in drinking water of 1.5 mg /L [2]. In India acceptable limits of Cu is 3mg/L [3]. Therefore, the concentrations of copper must be reduced to levels that satisfy environmental regulations for various bodies of water. Conventional treatment methods for heavy metals containing wastewater treatment include chemical precipitation, ultrafiltration, solvent extraction, ion exchange, reverse osmosis and adsorption. Among these techniques, adsorption is one of the most economically favorable and technically simple method [4]. Many heavy metal adsorption studies have focused on the application of activated carbons [5-6]. However, owing to the high cost and difficult procurement of activated carbon, efforts are being directed towards finding efficient and low cost adsorbent materials. A number of researchers have utilised wide variety of adsorbents to remove heavy metal ions from aqueous solutions. Some of the recent developments include adsorbents like sawdust [7], ca-kaolinite [8], Fithian illite [9], fly ash [10], baggase [11], activated carbon-zeolite composite [12], zeolite A [13], fertilizer plant waste slurry [14], modified clay [15], biosorbents like cassava waste [16], Arca [17], Lentil shell [18], Pine cone powder [19], Spent grain [20], crushed brick [21] etc. for the removal of copper ions from aqueous solutions.

In this study, the alluvial soil which was obtained from the river Bhagirathi, West Bengal, India will be investigated as a potential and low cost adsorbent for the removal of Cu^{2+} ions from aqueous solutions. The objective of the present work was to study the possibility of utilizing alluvial soil of Bhagirathi River (ASBR) as a sorbent for removing copper ions from aqueous solutions. The effects of adsorbent dose, initial copper concentration, contact time, stirring rate, temperature and pH on copper adsorption were investigated. Adsorption kinetics, isotherms and thermodynamic parameters were also evaluated and reported.

2. Materials and Methods

2.1. Preparation of the synthetic sample

All the reagents used for the current investigation were of GR grade from E. Merck Ltd., India. Copper sulphate ($\text{CuSO}_4 \cdot 5\text{H}_2\text{O}$) stock solution of 100 mg/L concentration was prepared and the working solutions were made by diluting the former with double distilled water. The range in concentrations of copper (II) ions prepared from standard solution varied between 10 to 40 mg/L. Before mixing the adsorbent, the pH of each copper solution was adjusted to the required value by 0.1 M NaOH or 0.1 M HCl solution.

2.2. Adsorbent collection and preparation

Alluvial soil used in this study was collected from the banks of river Bhagirathi owing to its high alluvial soil content and low permeability. The Bhagirathi River is one of the main rivers in Murshidabad, Burdwan, Nadia and Hooghly districts in the Indian state of West Bengal. The alluvial soil sample was not purified prior to usage. It was initially sun-dried for 7 days followed by drying in hot air oven at $383 \pm 1\text{K}$ for 2 days. The dried soil was crushed and sieved to give a fraction of 250 mesh screen and then stored in sterile, closed glass bottles and used as an adsorbent.

2.3. Analysis

Adsorbent characterization was performed by means of spectroscopic and quantitative analysis. The surface area of the adsorbent (ASBR) was determined by Quantachrome surface area analyzer (model- NOVA 2200C). Alumina was estimated by wet chemical analysis method [22]. The pH of the solution was measured using pH meter (Systronic 6.3 digital pH meter). The pH of aqueous slurry was determined by soaking 1g of ASBR in 50 ml distilled water, stirred for 24 h and filtered and the final pH was measured. The physico-chemical characteristics of the adsorbent were determined using standard procedures [23]. The % of clay, silt, and sand was determined by hydrometric method [23]. The cation exchange capacity (CEC) of the alluvial soil sample was determined by the ammonium acetate method [24]. The concentrations of sodium and potassium were estimated by Flame Photometer (Model No. SYSTRONICS 126) while magnesium, calcium and residual copper (II) concentration were determined by Atomic absorption spectrophotometer (Model No. GBC HG 3000). For stirring purpose magnetic stirrer (TARSONS, Spinot digital model MC02, CAT No. 6040, S. No. 173) is used. The pH of zero-point charge or pH_{ZPC} was determined based on the previous method [25]. The Fourier transform infrared (FTIR) spectra of ASBR before and after copper adsorption were recorded with Fourier transform infrared spectrophotometer (PERKIN-ELMER, FTIR, Model-RX1 Spectrometer, USA) in the range of $400\text{--}4,000\text{ cm}^{-1}$. X-ray diffraction analysis of the adsorbent was carried out using X-ray diffractometer equipment (Model Philips PW 1710) with a Cobalt target at 40 kV. In addition, scanning electron microscopy (SEM) analysis was carried out using a scanning electron microscope (HITACHI, S-530, Scanning Electron Microscope and ELKO Engineering, B.U. BURDWAN) at 10 kV to study the surface morphology of the adsorbent.

2.4. Batch Adsorption procedure

The batch tests were carried out in glass-stoppered, Erlenmeyer flasks with 50 mL of working volume, with a concentration of 10 mg/L. A weighed amount (2.0 g) of adsorbent was added to the solution. The flasks were agitated at a constant speed of 750 rpm for 2 h in a magnetic stirrer at $303 \pm 1\text{K}$. The influence of pH (2.0–8.0), initial copper concentration (10, 20, 30, 40 mgL^{-1}), contact time (10, 20, 30, 40, 60, 90, 120, 150 min), adsorbent dose (0.5, 1, 2, 2.5 g/50 ml), and temperature (303, 308, 313, 318, 323, 328 K) were evaluated during the present study. Samples were collected from the flasks at predetermined time intervals for analyzing the residual copper concentration in the solution. The residual amount of copper in each flask was investigated using atomic absorption spectrophotometer. The amount of copper ions adsorbed in milligram per gram was determined by using the following mass balance equation:

$$q_e = \frac{(C_i - C_e)V}{m} \quad (1)$$

where C_i and C_e are copper concentrations (mg/L) before and after adsorption, respectively, V is the volume of adsorbate in liter and m is the weight of the adsorbent in grams. The percentage of removal of copper ions was calculated from the following equation:

$$\text{Removal (\%)} = \frac{(C_i - C_e)}{C_i} \times 100 \quad (2)$$

Control experiments, performed without the addition of adsorbent, confirmed that the sorption of copper on the walls of flasks was negligible.

3. Results and Discussion

3.1. Characterization of ASBR

The ASBR was found to be stable in water, dilute acids and bases. The adsorbent behaves as neutral at pH zero charge. To understand the adsorption mechanism, it is necessary to determine the point of zero charge (pH_{zpc}) of the adsorbent. Adsorption of cation is favored at pH > pH_{zpc}, while the adsorption of anion is favored at pH < pH_{zpc} [25]. The point of zero charge is 4.75 irrespective of difference in concentration of HNO₃ used (Fig. 1). The physico-chemical properties of ASBR are summarized in Table 1.

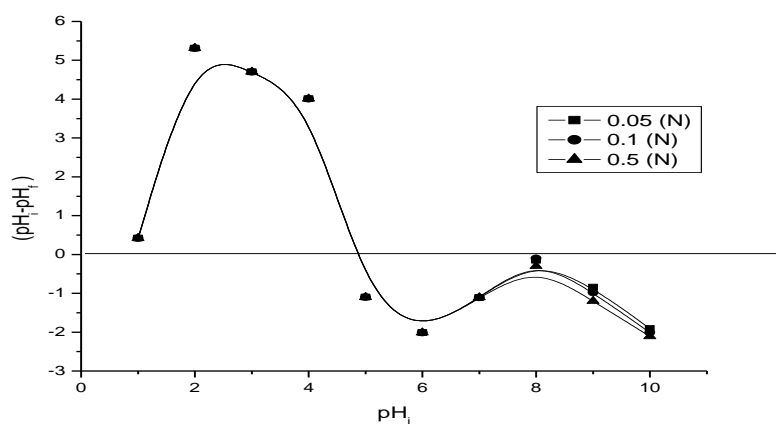


Figure 1: pH of zero point charge of ASBR (experimental conditions: adsorbent dose: 1.5 g in 100 ml, Temperature: 308K).

Table 1: Characteristics of ASBR

Analysis	Value
pH _{zpc}	4.75
Specific gravity	0.81
Moisture content (%)	0.53
Bulk density (g cm ⁻³)	1.351
Particle density (g cm ⁻³)	2.44
Porosity (%)	44.63
Clay (%)	3.08
Silt (%)	9.1
Sand (%)	81
Al ₂ O ₃ (%)	6.8
Conductivity (μS/cm)	2.0
BET surface area (m ² /g)	6.8
Micropore area (%)	32.5
Cation exchange capacity (meq g ⁻¹)	48
Na ⁺ (mg L ⁻¹)	61.15
K ⁺ (mg L ⁻¹)	16.7
Ca ²⁺ (mg L ⁻¹)	0.4
Mg ²⁺ (mg L ⁻¹)	11.6
PO ₄ ³⁻ (mg L ⁻¹)	0.817

The FTIR spectrum of ASBR was recorded to obtain the information regarding the stretching and bending vibrations of the functional groups which are involved in the adsorption of the adsorbate molecules. The FTIR spectra of ASBR before and after adsorption displayed a number of adsorption peaks, indicating a complex nature of the adsorbent (Fig. 2 and Fig. 3). The FTIR spectral analysis of ASBR before treatment shows distinct peaks at 3438, 2924, 2854, 1636, 1024, 778, 528, and 475 cm⁻¹. The broad and strong band at 3438 cm⁻¹ indicates the presence of -OH stretching. Two sharp peaks observed at 2924 and 2854 cm⁻¹ could be assigned to asymmetric and symmetric CH₂ group. The variable

peak at 1636 cm^{-1} was attributed to stretching vibration of $\text{C}=\text{C}$ alkene group. The characteristic band at 1024 cm^{-1} corresponds to $\text{C}-\text{O}$ stretching vibration. The peaks at 528 cm^{-1} and 778 cm^{-1} show the presence of $\text{C}-\text{Br}$ stretching and $\text{C}-\text{Cl}$ stretching vibration. Hence FTIR spectral analysis demonstrates the existence of negatively charged groups like $-\text{CH}_2$, $-\text{OH}$, $-\text{Cl}$, $-\text{Br}$ on the surface of ASBR. It is clearly shown in Fig. 3 that the intensity for copper-loaded ASBR was slightly lower than ASBR and there were some shifts in wave numbers after copper adsorption. Strong absorption band at 3438 cm^{-1} (indicative of $-\text{OH}$ stretching vibrations) shifted to 3422 cm^{-1} after copper adsorption. The band shift is also observed for $\text{C}-\text{O}$ group moving from 1024 cm^{-1} to 1082 cm^{-1} . The results suggest that copper interacts with $-\text{OH}$ and $\text{C}-\text{O}$ group present in ASBR.

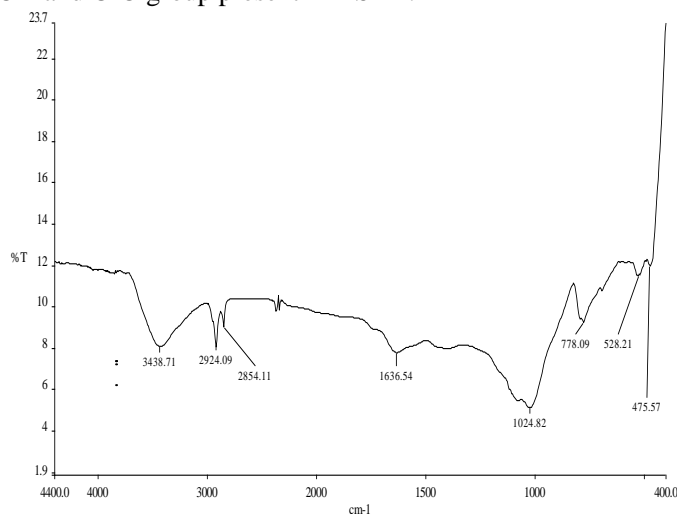


Figure 2: FTIR spectra of ASBR before adsorption of $\text{Cu}(\text{II})$ ions

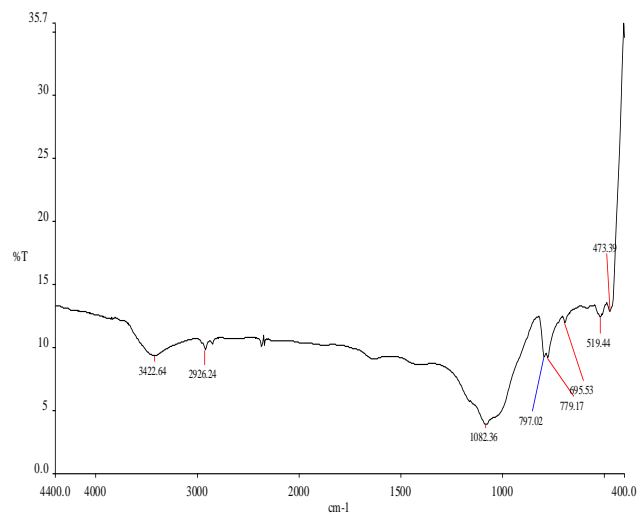


Figure 3: FTIR spectra of ASBR after adsorption of $\text{Cu}(\text{II})$ ions

Adsorption reaction may lead to changes in molecular and crystalline structure of the adsorbent and hence an understanding of the molecular and crystalline structures of the adsorbent and the resulting changes thereof would provide valuable information regarding adsorption reaction. Hence XRD patterns of the adsorbent before and after treatment with copper ions have been studied. Fig. 4 and Fig. 5 show the XRD patterns of the adsorbent before and after treatment with copper solutions. The XRD data for selective/predominant peaks are given in Table 2.

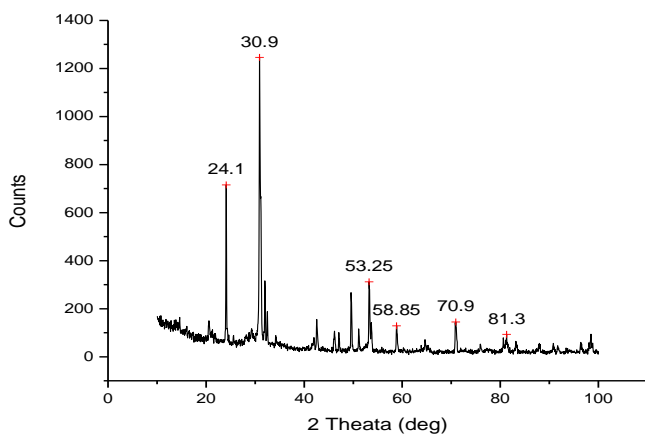


Figure 4: XRD pattern of the adsorbent before adsorption

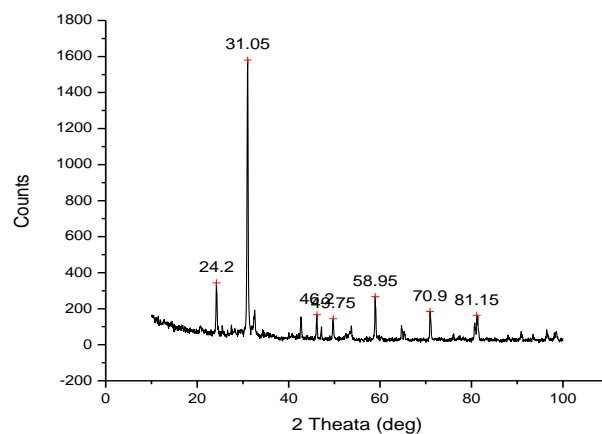


Figure 5: XRD pattern of the adsorbent after adsorption

From Fig. 5 it is clear that there was increase in the intensity of some of the diffraction peaks. The peak positions of the ASBR sample do not shift significantly. The intensity of the highly organized peaks are slightly diminished after the adsorption of copper ion. This due to the adsorption of copper ions on the upper layer of the crystalline structure of the ASBR surface by means of physisorption [26]. The above observation corroborated well with batch sorption experiments and thermodynamic results.

Table 2: X-ray diffraction details of the adsorbent before and after treatment with copper ions

Angle [2 Theta (deg)] Before adsorption	Peak height (Counts)
24.1	715
30.9	1246
42.4	146
46.23	100
49.5	213
53.25	312
58.85	129
70.9	146
After adsorption	
24.2	344
31.05	1580
42.7	142
46.2	142
49.6	129
53.3	80
58.95	267
70.9	142

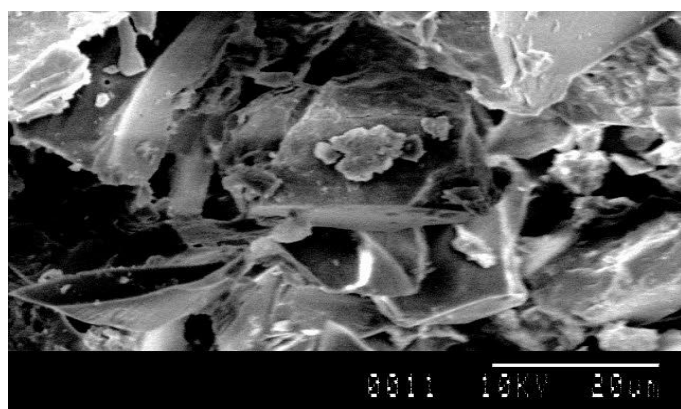


Figure 6: SEM image at 2000 magnification of ASBR before adsorption

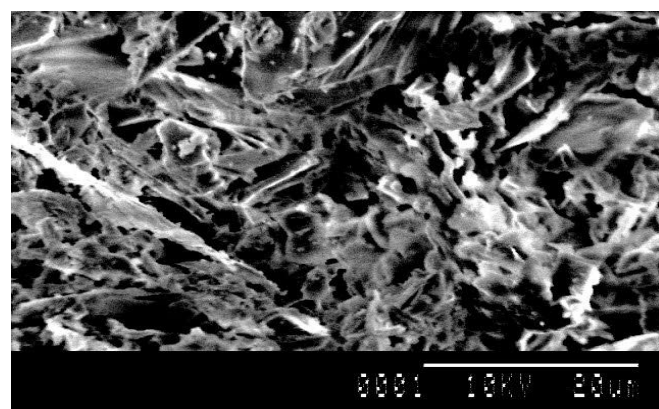


Figure 7: SEM image at 2000 magnification of ASBR after adsorption

3.2. Effect of copper concentration

The rate of adsorption is a function of the initial concentration of the adsorbate, which makes it an important factor to be considered for effective adsorption. The effect of different initial copper ion concentration on adsorption of copper ion onto ASBR is presented in Fig. 8. It shows that the increase in initial concentration of copper (II) decreases the adsorption and increases the amount of metal uptake per unit weight of the adsorbent (mg/g). The percentage decrease is between 99.5 % (0.24875 mg/g) and 83 % (0.835 mg/g) where the initial concentration increased between 10 and 40 mg/L. This is due to the fact that as concentration increases more copper ions are available for sorption on surfaces hence competition from other ions decreases for sorption on the same sites. A similar trend was observed for the adsorption of Cu (II) by sawdust [27].

3.3. Effect of sorbent dosage

In this study, five different adsorbent dosages were selected ranging from 0.5 to 2.5 g while the copper concentration was fixed at 10 mg/L. The results are presented in Fig. 9. It was observed that percentage of copper ion removal increased with increase in adsorbent dose. Such a trend is mostly attributed to an increase in the sorptive surface area and the availability of more active binding sites [28]. However, the adsorption capacity showed an opposite trend. As the adsorbent dosage was increased from 0.5 to 2.5 g, the adsorption capacity reduced to 0.34 and 0.19 mg g⁻¹,

respectively. This may be due to the decrease in total adsorption surface area available to copper ion resulting from overlapping or aggregation of adsorption sites [29-30]. Thus with increasing the adsorbent mass the amount of copper ion adsorbed onto unit mass of adsorbent gets reduced, thus causing a decrease in q_e value with increasing adsorbent mass concentration. This is a clear indication that an increase in adsorbent dosage results in higher number of unoccupied binding site in ASBR. Furthermore maximum copper ion removal (99.5%) was recorded by 2.0 g ASBR and further increase in adsorbent dose did not significantly change the adsorption yield. This is due to the non-availability of active sites on the adsorbent and establishment of equilibrium between the copper ion on the adsorbent and in the solution. Similar results have been reported for Cu (II) adsorption [31-32].

3.4. Effect of pH

The pH of the aqueous solution is an important controlling parameter in the adsorption process due to its influence on the degree of ionization of functional groups (carboxylate, hydroxyl, sulfate, phosphate etc) and different ionic forms of copper [32]. The effect of pH on the removal efficiency of copper ion was studied at different pH ranging from 2.0 to 8.0. Results are shown in Fig. 10. It was observed that a sharp increase in the copper ion removal occurred when the pH value of the solutions changed from 2.0 to 4.0 and after 4.0 a plateau is obtained.

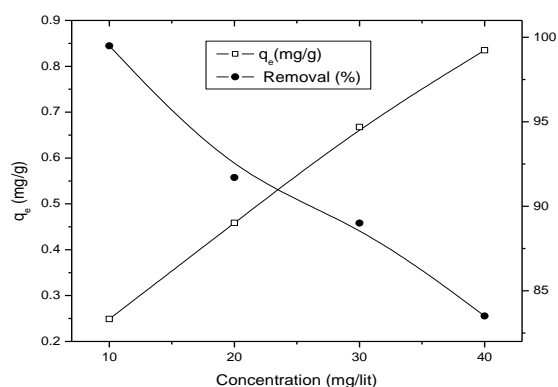


Figure 8: Effect of initial concentration on copper adsorption (experimental conditions: adsorbent dose: 2 g/ 50 ml, stirring rate: 750 rpm, pH: 6.0, temperature: 308K, contact time: 2 h).

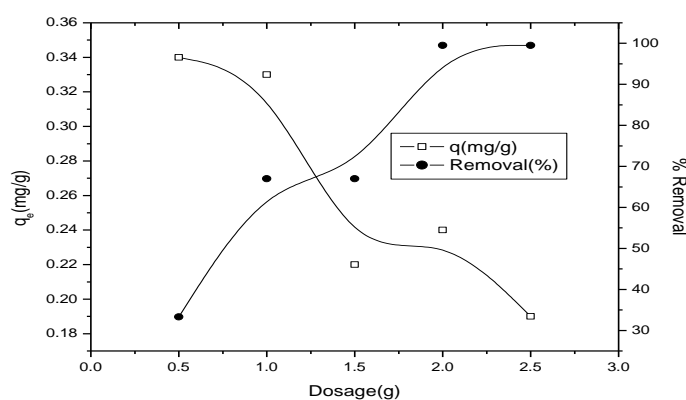
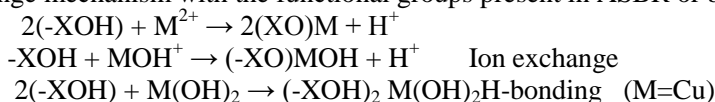


Figure 9: Effect of sorbent dosage on copper adsorption (experimental conditions: initial concentration: 10mg/L, stirring rate: 750 rpm, pH 6.0, temperature: 308K, contact time: 2 h).

The maximum adsorption of copper ion occurred in the pH range 4.0 to 6.0. So pH 6.0 was selected as optimum pH for copper ion adsorption onto ASBR. From pH 6 onwards a steady decrease of adsorption of copper ion were recorded. Again the FTIR spectral analysis indicates the involvement of $-OH$ functional group in the adsorption process of copper ion onto ASBR. This $-OH$ group is protonated at pH values lower than 2.0 and thereby restrict the approach of positively charged metal ions to the surface of the adsorbent which results in lower uptake of metal. Again decreasing in adsorption at high pH may be due to the formation of soluble hydroxy complexes [33]. At pH 6 there are three species present in solution as suggested by Elliot and Huang [34]: Cu^{2+} in very small quantity and $Cu(OH)^+$ and $Cu(OH)_2$ in large quantities. Therefore, the specific sorption of these copper species onto ASBR may be modeled by ion exchange mechanism with the functional groups present in ASBR or by hydrogen bonding as shown below



where X represents the matrix of ASBR.

Quite similar results have been reported in literature for adsorption of copper ions [35-36].

3.5. Effect of Contact Time

The effect of contact time on the removal of copper ion is shown in Fig. 11. The removal rate was rapid initially and then gradually diminished to attain an equilibrium time beyond which there was no significant increase in the rate of

removal. The equilibrium was nearly reached after 60 min for four different initial copper (II) ion concentrations. Hence, in the present work, 60 min was chosen as the equilibrium time. The fast adsorption rate at the initial stage may be explained by an increased availability in the number of active binding sites on the adsorbent surface. The sorption rapidly occurs and normally controlled by the diffusion process from the bulk to the surface. In the later stage the sorption is likely an attachment-controlled process due to less available sorption sites. Similar results have been reported in literature for Cu (II) adsorption [36-39].

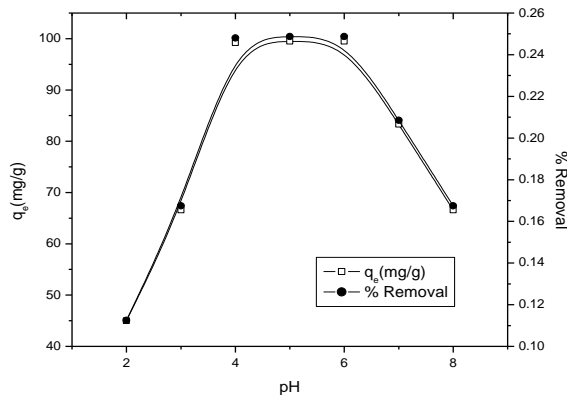


Figure 10: Effect of pH on copper adsorption (experimental conditions: initial concentration: 10mg/L, adsorbent dose: 2 g/ 50 ml, stirring rate: 750 rpm, temperature: 308K, contact time: 2 h).

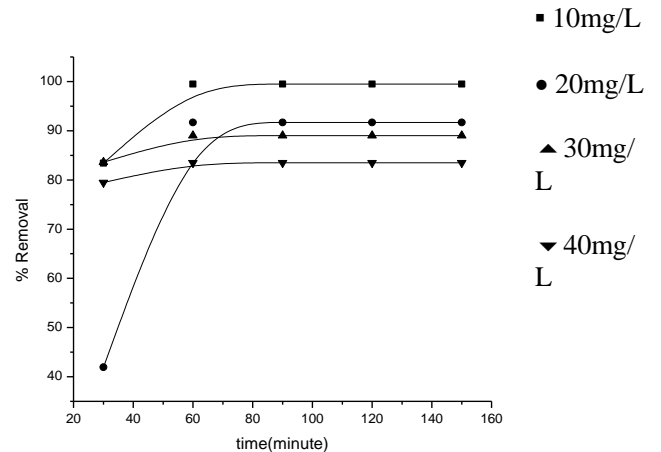


Figure 11: Effect of contact time on copper adsorption (experimental conditions: adsorbent dose: 2 g/ 50 ml, stirring rate: 750 rpm, pH: 6.0, temperature: 308K).

3.6. Effect of stirring rate

The effect of stirring rate on the removal of copper ion is shown in Fig. 12. There is a steady increase in the percentage of copper ion removal with increase in the stirring rate from 250 to 1000 rpm. Maximum removal of copper ions occurs when stirring rate is 750 rpm and thereafter the removal is almost constant and the stirring rate of 750 rpm was selected in subsequent analysis. The increase in removal percentage at a higher stirring rate could be explained in terms of boundary layer thickness. With increasing the stirring rate a good degree of mixing could be achieved and the thickness of boundary layer around the adsorbent particles could be reduced. Therefore the concentrations of copper ions would be increased near the adsorbent surface. A higher stirring rate would also ensure better mass transfer of copper ions from bulk solution to the surface of the adsorbent and shortened the adsorption equilibrium time.

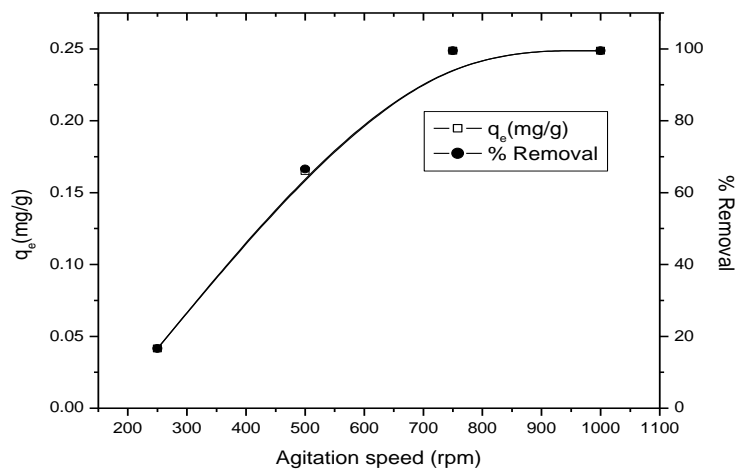


Figure 12: Effect of stirring rate on adsorption of copper by ASBR (experimental conditions: initial concentration: 10mg/L, adsorbent dose: 2 g/ 50 ml, pH: 6.0, temperature: 308K, contact time: 60 min).

3.7. Adsorption isotherms

An adsorption isotherm represents the equilibrium relationship between the adsorbate concentration in the liquid phase and that on the adsorbents surface at a given condition. Sorption studies were performed over an initial concentration range of 10-40 mg/L. A number of isotherms have been developed to describe equilibrium relationships. In the present study, Langmuir, Freundlich, Temkin, Dubinin-Radushkevich (D-R) and BET models were used to describe the equilibrium data.

The Langmuir isotherm model [40] was used to describe observed sorption phenomena and suggests that uptake occurs on a homogeneous surface by monolayer sorption without interaction between adsorbed molecules. The linear form of the equation can be written as

$$\frac{1}{q_{eq}} = \frac{1}{q_{max} K_L C_e} + \frac{1}{q_{max}} \quad (3)$$

Where C_e is the equilibrium concentration of Cu(II) (mg/L), q_{eq} is the amount of metal adsorbed per specific amount of adsorbent (mg/g), q_{max} is the maximum adsorption capacity (mg/g), and k_L is an equilibrium constant (L/mg) related to energy of adsorption which quantitatively reflects the affinity between the adsorbent and adsorbate. Where q_{max} and k_L can be determined from the linear plot of $1/q_{eq}$ vs $1/C_e$ (Figure not shown). The shape of the Langmuir isotherm can be used to predict whether a sorption system is favorable or unfavorable in a batch adsorption process. The essential features of the isotherm can be expressed in terms of a dimensionless constant separation factor (R_L) that can be defined by the following relationship [41]

$$R_L = \frac{1}{1 + K_L C_i} \quad (4)$$

Where C_i is the initial concentration (mg/L) and k_L is the Langmuir equilibrium constant (L/mg). The value of separation parameter R_L provides important information about the nature of adsorption. The value of R_L indicated the type of Langmuir isotherm to be irreversible ($R_L=0$), favourable ($0 < R_L < 1$), linear ($R_L=1$) or unfavourable ($R_L > 1$). It can be explained apparently that when $k_L > 0$, sorption system is favorable [42]. The evaluated constants are given in Table 3. Freundlich isotherm model proposes a monolayer sorption with a heterogeneous energetic distribution of active sites, accompanied by interactions between adsorbed molecules. The linear form of the equation [43] can be written as:

$$\log q_{eq} = \log K_F + \frac{1}{n} \log C_e \quad (5)$$

Where, K_F is the maximum adsorption capacity (mg/g) and n is related to the adsorption intensity of the adsorbent. Where, K_F and $1/n$ can be determined from the linear plot of $\log q_{eq}$ versus $\log C_e$ (Figure not shown). The evaluated constants are given in Table 3.

Unlike the Langmuir and Freundlich equation, the Temkin isotherm takes into account the interactions between adsorbents and metal ions to be adsorbed and is based on the assumption that the free energy of sorption is a function of the surface coverage [42]. The linear form of the Temkin isotherm is represented as:

$$q_e = B \ln A + B \ln C_e \quad (6)$$

Where C_e is concentration of the adsorbate at equilibrium (mg/L), q_e is the amount of adsorbate adsorbed at equilibrium (mg/g), $RT/b_T = B$ where T is the temperature (K), and R is the ideal gas constant ($8.314 \text{ J mol}^{-1} \text{ K}^{-1}$) and A and b_T are constants. A plot of q_e versus $\ln C_e$ enables the determination of constants A and B . The constant B is related to the heat of adsorption and A is the equilibrium binding constant (L/min) corresponding to the maximum binding energy. The values of A and B are given in Table 3.

The Dubinin-Radushkevich model [44] was chosen to estimate the apparent free energy of adsorption. The linear form of D-R isotherm equation is represented as:

$$\ln q_e = \ln q_m - \beta \epsilon^2 \quad (7)$$

$$\text{Where } \epsilon = RT \ln \left(1 + \frac{1}{C_e} \right) \quad (8)$$

where q_m is the theoretical saturation capacity (mol/g), β is a constant related to the mean free energy of adsorption per mole of the adsorbate (mol^2/J^2), and ϵ is the polanyi potential, C_e is the equilibrium concentration of adsorbate in

solution (mol/L), R (J/mol/K) is the gas constant and T(K) is the absolute temperature. The D-R constants q_m and β were calculated from the linear plots of $\ln q_e$ versus ϵ^2 (Figure not shown) and are given in Table 3. The constant β gives an idea about the mean free energy E (kJ/mol) of adsorption per molecule of the adsorbate when it is transferred to the surface of the solid from infinity in the solution and can be calculated from the relationship [45]

$$E = \frac{1}{\sqrt{2\beta}} \quad (9)$$

If the magnitude of E is between 8 and 16 kJ mol⁻¹, the sorption process is supposed to proceed via chemisorption, while for values of E < 8 kJ mol⁻¹, the sorption process is of physical nature [45].

The BET isotherm is a S-shaped isotherm [46]. The isotherm constants, K_B and q_m were calculated for copper ion sorption by the following equation:

$$\frac{C_e}{(C_s - C_e)q_e} = \frac{1}{K_B q_m} + \left(\frac{K_B - 1}{K_B q_m} \right) \frac{C_e}{C_s} \quad (10)$$

where C_e is the concentration of solute remaining in solution at equilibrium (mg/L), C_s the saturation concentration of solute (mg/L), q_e the amount of solute adsorbed per unit weight of adsorbent (mg/g), q_m the amount of solute adsorbed per unit weight of adsorbent in forming a complete monolayer on the surface (mg/g) and K_B is the constant expressive of energy of interaction with the surface. A plot of $\frac{C_e}{(C_s - C_e)q_e}$ vs. $\frac{C_e}{C_s}$ would yield a straight line, from the slope

and intercept of which q_m and K_B can be determined. The values of q_m and K_B for the adsorption of Cu (II) on ASBR are given in Table 3.

3.8. Error analysis

Due to the inherent bias resulting from linearization, four different error functions of non-linear regression basin [sum of the square of the errors (SSE), sum of the absolute errors (SAE), Marquardt's percent standard deviation (MPSD) and chi-square (χ^2)] were employed in this study to find out the best-fit isotherm model to the experimental equilibrium data.

SSE is given as:

$$SSE = \sum_{i=1}^n (q_{e,estm} - q_{e,exp})_i^2 \quad (11)$$

Here, $q_{e,estm}$ and $q_{e,exp}$ are, respectively, the estimated and the experimental value of the equilibrium adsorbate solid concentration in the solid phase (mg/g), and n is the number of the data point.

SAE is given as:

$$SAE = \sum_{i=1}^n |q_{e,estm} - q_{e,exp}|_i \quad (12)$$

MPSD has been used by a number of researchers in the field to test the adequacy and accuracy of the model fit with the experimental data. This error function is given as:

$$MPSD = 100 \sqrt{\frac{1}{n-P} \sum_{i=1}^n \left(\frac{q_{e,exp} - q_{e,estm}}{q_{e,exp}} \right)_i^2} \quad (13)$$

Chi-square (χ^2) is given as:

$$\chi^2 = \sum_{i=1}^n \left[\frac{(q_{e,exp} - q_{e,estm})^2}{q_{e,estm}} \right]_i \quad (14)$$

The respective values are given in the Table 3.

As shown in Table 3, it was observed that both the Langmuir and Freundlich isotherm was better fitted with the experimental equilibrium adsorption data than the Dubinin-Radishkevich, Tempkin and BET isotherm equation for Cu (II) sorption according to the values of R^2 , MPSD, χ^2 , SSE and SAE. It was also seen from Table 3 that the Langmuir maximum adsorption capacity q_{max} (mg/g) is 0.633 and the equilibrium constant k_L (L/ mg) is 12.88. The Freundlich constant K_F indicates the sorption capacity of the sorbent and the value of K_F is 0.48 mg/g. Furthermore, the value of 'n' at equilibrium is 4.2. The value of n lies between 1 and 10 indicating favorable adsorption [47]. The separation

factor (R_L) values are 0.007, 0.003, 0.002 and 0.001 while initial Cu (II) concentrations are 10, 20, 30 and 40 mg/L, respectively. All the R_L values were found to be less than one and greater than zero indicating the favorable sorption of Cu (II) onto ASBR. From D-R isotherm the value of the adsorption energy was found to be 5.64 kJ/mol. The energy value for the Cu (II) ions sorption on the ASBR indicates that the sorption process is physisorption. The Temkin constant, b_T related to heat of sorption for copper ions was found to be 14.76. It has been reported that the typical range of bonding energy for ion-exchange mechanism is 8-16 kJ/mol [48]. The value in this study indicates a weak interaction between sorbate and sorbent, supporting an ion-exchange mechanism for the present study. The effectiveness of ASBR as an adsorbent for copper adsorption was also compared with other reported adsorbents. The maximum adsorption capacity obtained in this study is comparable with other adsorbents as shown in Table 4.

Table 3: Adsorption isotherm constants for adsorption of copper (II) onto ASBR

Adsorption isotherms	Parameters		R^2	χ^2	SSE	SAE	MPSD
Langmuir isotherm	q_{max} (mg/g)	0.633	0.905	2.277	0.375	1.2172	20.559
	K_L (L/mg)	12.88					
Freundlich isotherm	K_F (mg/g)(L mg ⁻¹) ^{1/n}	0.48	0.9479	2.529	0.385	1.2671	21.28
	n	4.2					
Temkin isotherm	B (mg/g)	0.1763	0.8033	2.987	0.4018	1.344	22.37
	A	68.03					
D-R isotherm	q_m (mg/g)	0.642	0.79	2.985	0.42	1.3591	22.58
	β (mol ² kJ ⁻²)	0.0157					
	E(kJ mol ⁻¹)	5.64					
BET	q_m (mg/g)	0.7232	0.8744	8.657	0.492	1.7611	29.83
	K_B	36.58					

Table 4: A comparisons of maximum adsorption capacities for copper ions by different adsorbents

Adsorbent	q_{max} (mg/g)	pH	T(K)	Reference
Sphagnum peat moss	12.60	5	298	[49]
Neurospora crassa	12.30	5	298	[50]
Saccharomyces cerevisiae	10.72	6	298	[51]
Cercis siliquastrum	9.35	4	NA	[52]
Activated carbon	9.22	NA	293	[53]
Modified carrot residue	8.74	5.2	293	[54]
Puracite C-104 ion-exchange	7.92	4.5	298	[55]
Modified oak sawdust	3.60	4	313	[56]
Potato peels	0.38	6	303	[57]
Periwinkle shell carbon	0.07	8	NA	[58]
Powdered limestone	0.29	7	298	[59]
A. Spinosus	0.206	NA	NA	[60]
Gonoderma	0.375	NA	NA	[61]
ASBR	0.63	6	313	This study

3.9. Adsorption Kinetics Modeling

The rate of adsorption and possible adsorption mechanism of copper onto ASBR was analyzed using Lagergren first order [62], pseudo-second order [63], Intraparticle diffusion [64], Elovich [65] and surface mass transfer model [66]. The Lagergren first order rate equation is represented as:

$$\log(q_e - q_t) = \log q_e - \frac{k_1 t}{2.303} \quad (15)$$

Where q_e and q_t are the amounts of copper adsorbed (mg/g) at equilibrium and at time t , respectively and k_1 is the Lagergren rate constant of first order adsorption (min^{-1}). Values of q_e and k_1 at different concentrations were calculated from the slope and intercept of the plots of $\log (q_e - q_t)$ versus t (Figure not shown). The respective values are given in the Table 5.

The second order kinetic model is represented as

$$\frac{t}{q_t} = \frac{1}{k_2 q_e^2} + \frac{t}{q_e} \quad (16)$$

Where k_2 is the rate constant of second order adsorption (g/mg/min). Values of k_2 and q_e were calculated from the plots of t/q_t versus t (Fig. 13). The respective values are given in the table 5. Furthermore the plot of t/q_t versus t at different temperatures is shown in Fig. 14 and the pseudo-second-order model constants were presented in the Table 5. Again from the pseudo-second-order kinetic parameters, the initial adsorption rate, h ($\text{mg g}^{-1} \text{min}^{-1}$) [67] at different temperatures was calculated using Eq. (17) and are presented in Table 6:

$$h = k_2 q_e^2 \quad (17)$$

The most commonly used technique for identifying the mechanism involved in the adsorption process is by using intra-particle diffusion model as (Weber and Morris model):

$$q_t = K_d t^{1/2} + I \quad (18)$$

Here, I is the intercept and K_d is the intra-particle diffusion rate constant. The intercept of the plot reflects the boundary layer effect. Larger the intercept, greater is the contribution of the surface sorption in the rate controlling step. If the regression of q_t against $t^{1/2}$ will be linear and the line will pass through the origin then intra-particle diffusion was the only rate limiting parameter controlling the process. Otherwise, some other mechanism is also involved. Fig. 15 presents intra-particle plot for copper (II) onto ASBR. The figure shows three distinct regions, the initial curved region corresponds to the external surface uptake, the second stage relates the gradual uptake reflecting intraparticle diffusion as the rate limiting step and final plateau region indicates equilibrium uptake. The diffusion rate parameters were shown in Table 5. The k_{id} value was higher at the higher concentrations.

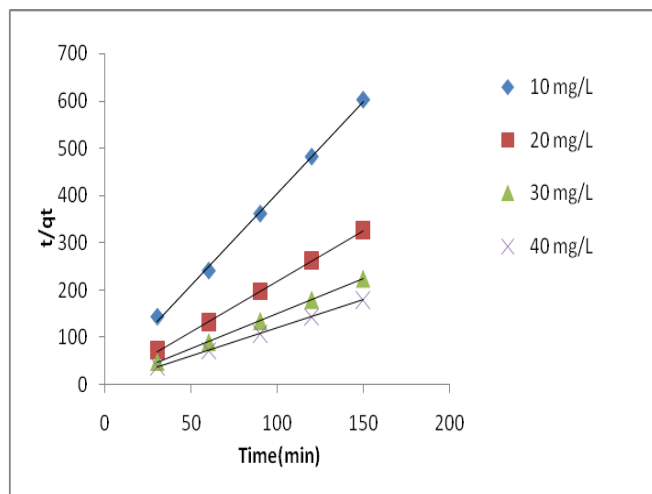


Figure 13: Second order plots of copper adsorption onto ASBR (experimental conditions: temperature: 308 K, adsorbent dose: 2 g/ 50 ml, agitation speed: 750 rpm, pH: 6.0)

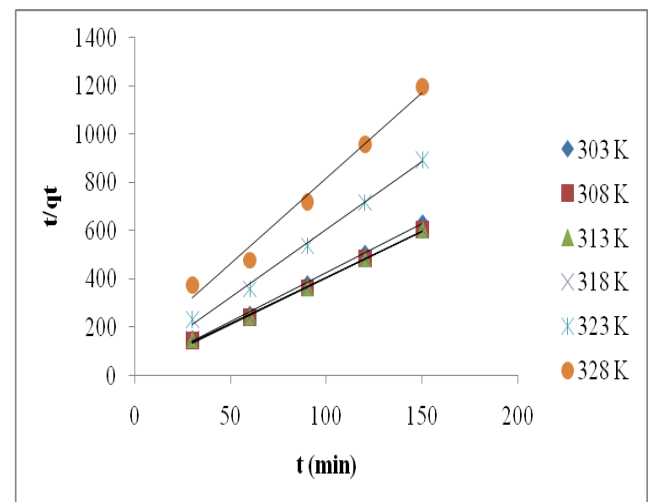


Figure 14: Pseudo second- order kinetic plots for adsorption of copper onto ASBR at different temperatures (experimental conditions: initial copper ion concentration: 10 mg/ L, adsorbent dose: 2 g/ 50 ml, agitation speed: 750 rpm, pH: 6.0).

Mass transfer analysis for the removal of copper was carried out using the kinetic model which describes the transfer of adsorbate in solution. The model is expressed as:

$$\ln \left(\frac{C_t}{C_0} - \frac{1}{1 + mk_L} \right) = \ln \frac{mk_L}{1 + mk_L} - \frac{1 + mk_L}{mk_L} \beta_L S_s t \quad (19)$$

where C_t is the concentration (mg/L) after time t , C_o is the initial concentration (mg/L), m is the mass of adsorbent per unit volume of particle-free adsorbate solution (g/L), β_L is the mass transfer coefficient (cm/s), k_L is the constant obtained from the Langmuir isotherm equation (L/g), and S_s is the outer surface of adsorbent per unit volume of particle free solution (cm⁻¹), given as:

$$S_s = \frac{6m}{D_a d(1 - \varepsilon)} \quad (20)$$

Where D_a is the particle mean diameter (cm), d is the density of the adsorbent (g/cm³) and ε is the porosity of the adsorbent. The results are showing in Fig. 16. The plot of $\ln\left(\frac{C_t}{C_o} - \frac{1}{1 + mk_L}\right)$ versus t for gives a straight line and thus confirms the validity of the equation for the present system. The value of β_L for different initial concentrations was determined from the slope and intercept of the plots and are shown in Table 5.

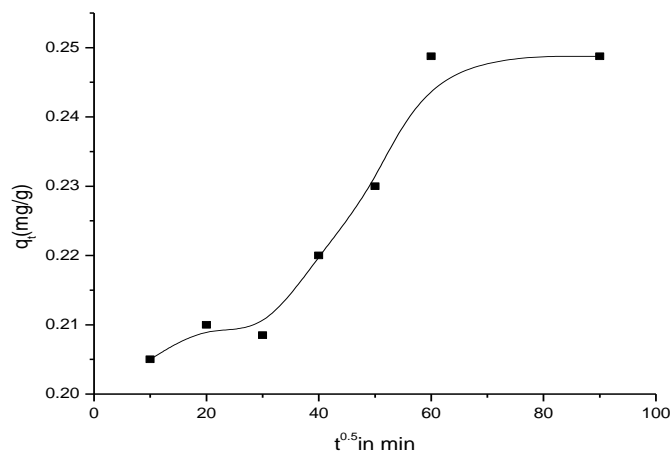


Figure 15: Intraparticle diffusion effect on the adsorption of copper onto ASBR (experimental conditions: initial copper ion concentration: 10 mg /L, adsorbent dose: 2 g/ 50 ml, agitation speed: 750 rpm, pH: 6.0)

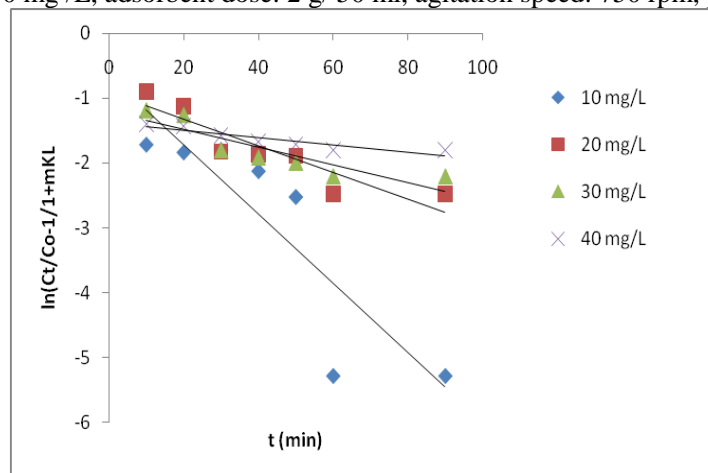


Figure 16: Mass transfer plot for the adsorption of copper on ASBR (experimental conditions: adsorbent dose: 2 g/ 50 ml, agitation speed: 750 rpm, pH: 6.0, temperature: 308 K).

The Elovich equation is useful in describing adsorption on highly heterogeneous surfaces. The Elovich kinetic model is represented as:

$$q_t = \frac{1}{\beta} \ln(\alpha\beta) + \frac{1}{\beta} \ln t \quad (21)$$

Where α is the initial sorption rate constant (mg/g.min), and the parameter β is related to the extent of surface coverage and activation energy for chemisorptions (g/mg). Both the kinetic constants (β and α) will be estimated from the slope and intercept of the plot q_t versus $\ln t$ (Fig.17). The corresponding values are represented in the Table 5.

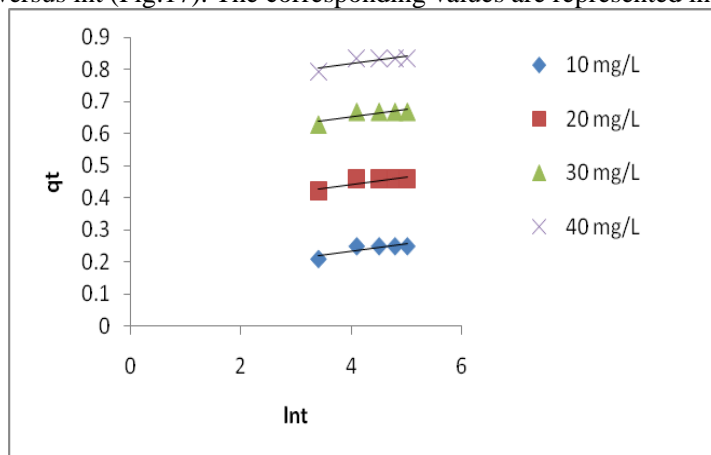


Figure 17: Elovich plots of copper adsorption onto ASBR (experimental conditions: temperature: 308 K, adsorbent dose: 2 g/ 50 ml, agitation speed: 750 rpm, pH: 6.0).

Table 5: Kinetic parameters for adsorption of copper (II) onto ASBR

Kinetic model	parameters	Concentration of copper (II) solution			
		10 mg/L	20 mg/L	30 mg/L	40 mg/L
	$q_{e,exp}$ (mg/g)	0.24875	0.4585	0.6675	0.8350
Pseudo-first-order	k_1 (min^{-1})	0.02	0.04	0.05	0.04
	$q_{e,cal}$ (mg/g)	0.06	0.23	0.28	0.15
	R^2	0.831	0.870	0.928	0.965
Pseudo-second-order	k_2 ($\text{g/mg}^{-1} \text{min}^{-1}$)	0.8025	0.9420	0.9507	1.66
	$q_{e,cal}$ (mg/g)	0.258	0.467	0.676	0.843
	R^2	0.998	0.999	0.999	0.999
Intraparticle diffusion	K_d ($\text{mg/g.min}^{1/2}$)	0.008	0.035	0.038	0.047
	I	0.17	0.192	0.411	0.497
	R^2	0.787	0.917	0.903	0.788
Surface mass transfer	β_L (cm/s)	2.326×10^{-6}	0.695×10^{-6}	0.33×10^{-6}	0.113×10^{-6}
	R^2	0.7697	0.8259	0.7808	0.8339
Elovich	α (g/min)	7.28	8.7×10^4	2.9×10^8	3.2×10^{11}
	B (g^{-1})	41.84	43.29	41.84	41.84
	R^2	0.70	0.70	0.70	0.70

Table 6 : Pseudo-second-order kinetic parameters at different temperatures

T(K)	$q_{e,cal}$ (mg g^{-1})	k_2 ($\text{g mg}^{-1} \text{min}^{-1}$)	h ($\text{mg g}^{-1} \text{min}^{-1}$)
303	0.245	0.836	0.05
308	0.2587	0.8025	0.05
313	0.259	0.72	0.048
318	0.2610	0.644	0.043
323	0.180	0.60	0.01
328	0.14	0.47	0.009

It is clear from the Table 5 that the pseudo- second-order kinetic model showed excellent linearity with high correlation coefficient ($R^2 > 0.99$) at all the studied concentrations in comparison to the other kinetic models. In addition the calculated q_e values also agree with the experimental data in the case of pseudo-second-order kinetic model. It is also observed from Table 6 that rate constant, k_2 decreased as the temperature increased indicating exothermic nature of adsorption of copper ion onto ASBR. Again as evident from Table 6, the initial adsorption rate, h , decreased with increase in temperature suggesting that adsorption of copper ion onto ASBR was not favorable at higher temperatures. Again as shown in Table 5 the external mass transfer coefficient ranges from $2.326 \times 10^{-6} \text{ cm s}^{-1}$ for 10 mg l^{-1} initial Cu (II) and $0.113 \times 10^{-6} \text{ cm s}^{-1}$ for 40 mg l^{-1} Cu(II) concentration. It was found that the external mass transfer coefficient decreased with increase in initial Cu(II) concentration. These results are consistent with previous studies on copper and mercury sorption onto chitosan [68].

3.10. Thermodynamic Parameters and Activation energy.

In order to study the feasibility of the adsorption process, the thermodynamic parameters such as free energy, enthalpy and entropy changes can be estimated from the following equations [69]:

$$K_c = \frac{C_{Ae}}{C_e} \quad (22)$$

$$\Delta G^0 = -RT \ln K_c \quad (23)$$

$$\log K_c = \frac{\Delta S^0}{2.303R} - \frac{\Delta H^0}{2.303RT} \quad (24)$$

Where C_e is the equilibrium concentration in solution in mg/L and C_{Ae} is the equilibrium concentration on the sorbent in mg/L and K_c is the equilibrium constant. The Gibbs free energy change (ΔG^0) at all temperatures was obtained from Eq. (23). The values of ΔH^0 and ΔS^0 were obtained from the slope and intercept of the plot $\log K_c$ against $1/T$ (Fig. not shown) and are listed in Table 7.

From the pseudo-second-order rate constant k_2 (Table 6), the activation energy E_a for the adsorption of copper ions on ASBR was determined using the Arrhenius equation:

$$\ln k = \ln A - \frac{E_a}{RT} \quad (25)$$

Where k is the rate constant, A is the Arrhenius constant, E_a is the activation energy (kJ mol^{-1}), R is the gas constant ($8.314 \text{ J mol}^{-1} \text{ K}^{-1}$) and T is the temperature (K). By plotting $\ln k$ versus $1/T$, E_a was obtained from the slope of the linear plot (Figure not shown).

Table 7: Thermodynamic and activation energy parameters for adsorption of copper onto ASBR

Temp.(K)	$\Delta G^0(\text{kJmol}^{-1})$	$\Delta H^0(\text{kJmol}^{-1})$	$\Delta S^0(\text{kJmol}^{-1})$	$E_a(\text{kJ mol}^{-1})$
		-56.80	-0.159	-17.63
303	-7.164			
308	-13.55			
313	-13.77			
318	-13.99			
323	-1.901			
328	-0.027			

From Table 7 it is clear that the reaction is spontaneous in nature as ΔG^0 values are negative at all the temperature studied. Increase in value of ΔG^0 with increase in temperature suggests that lower temperature makes the adsorption easier. It is of note that ΔG^0 up to -20 KJ/mol are consistent with electrostatic interaction between sorption sites and the metal ion (physical adsorption) while ΔG^0 values more negative than -40 KJ/mol involve charge sharing or transfer from the adsorbent surface to the metal ion to form a coordinate bond (chemical adsorption) [70]. The ΔG^0

values obtained in this study for copper ions are less negative than -20 KJ/mol, indicative that physical adsorption is the predominant mechanism in the sorption process. Again negative ΔH° value confirms that the sorption is exothermic in nature. The negative values of ΔS° suggest that the adsorption process is enthalpy driven. The magnitude of activation energy (E_a) can reveal important information on the mechanism of sorption reaction. Low E_a values usually indicate that adsorption is diffusion-controlled transport and physical adsorption process, whereas higher E_a values ranging from 8.4 to 83.7 kJ/mol would indicate that chemical reaction is the predominant process [71]. The E_a value was found to be -17.63 kJ mol⁻¹. The measured E_a value suggests that the adsorption is physisorption and diffusion controlled. The negative values of E_a indicate that lower solution temperature favors metal ion removal by adsorption onto the ASBR and the adsorption process is exothermic in nature [70].

3.11. Effect of co-ions on copper adsorption.

Actually, copper contaminated water contains several other ions that may influence the adsorption process. This study assessed copper adsorption behavior in the presence of 0.1 M salt solutions of sodium, calcium and aluminum, independently, at an initial copper concentration of 10 mg/L. The effect of these coexisting ions on copper removal is shown in Fig. 18. It was observed that copper removal decreased from 99.5% to 67% in the presence of sodium and to 34% in the presence of calcium and to 22% in the presence of aluminum. According to the Surface Chemistry Theory developed by Guoy and Chapman [72], when solid adsorbent is in contact with sorbate species in solution phase, they are bound to be surrounded by an electrical diffused double layer; the thickness of the layer is significantly expanded by the presence of electrolyte. Such expansion inhibits the adsorbent particles and Cu (II) from approaching. Copper removal in the presence of an ions increased in the order $Al^{3+} < Ca^{2+} < Na^{+}$. This correlates with the Z/r (charge/radius) values of the cations, which varies in the order $Al^{3+} > Ca^{2+} > Na^{+}$.

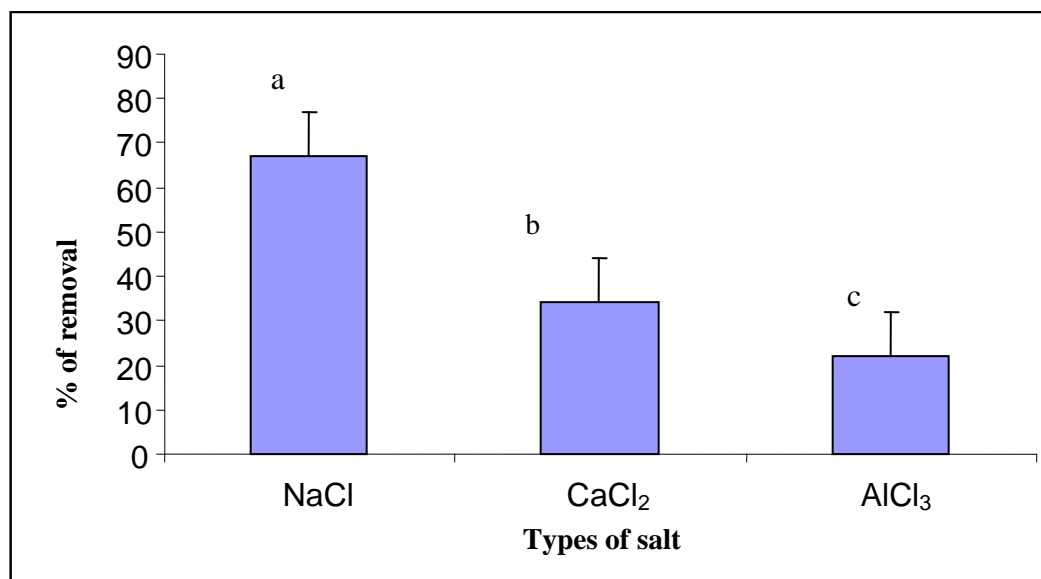


Figure 18: Effect of interfering ions for copper removal on ASBR (experimental conditions: initial copper ion concentration: 10 mg L⁻¹, adsorbent dose: 2 g/ 50 ml, agitation speed: 750 rpm, pH: 6.0 , Temperature: 308 K). Vertical bar with dissimilar letters are significantly different ($p < 0.05$)

Conclusions

In this study, natural alluvial soil of Bhagirathi river of Indian origin was tested and evaluated as a possible adsorbent for removal of copper from its aqueous solution using batch sorption technique. The adsorption process is also dependent on numerous factors such as the solution pH, adsorbent dosage, temperature, stirring rate, initial concentration and contact time. The percentage removal of copper ions decreased with an increase in the copper concentration while it increased with increase in contact time and adsorbent dose. The maximum removal was found between the pH ranges 2.0 - 6.0 . The isotherm study indicates that the sorption data can be modeled by both Langmuir and Freundlich isotherms. According to Dubinin-Radushkevich (D-R) isotherm model, adsorption of copper onto ASBR was physisorption. The adsorption kinetics followed pseudo-second-order kinetic model. Intra-particle diffusion was not the sole rate controlling factor. The activation energy of the adsorption process (E_a) was found to be -17.63 kJ mol⁻¹ by using the Arrhenius equation, indicating physisorption nature

of copper adsorption onto ASBR. Thermodynamic analysis suggests that the removal of copper from aqueous solution by ASBR was a spontaneous and exothermic process. The present findings suggest that ASBR may be used as an inexpensive and effective adsorbent without any treatment or any other modification for the removal of copper from aqueous solutions.

Acknowledgement

The authors are grateful to Dr. Alope Ghosh, Reader, Department of Chemistry, Burdwan University, West Bengal, India for recording FTIR data and they also extend their gratitude to Dr. Srikanta Chakraborty, Incharge of SEM, USIC, University of Burdwan, West Bengal for SEM study.

References

1. Abu Al-Rub, F.A., El-Naas, M.H., Ashour, I., Al-Marzouqi, M., *Process Biochem.* 41 (2006) 457
2. Ayhan, I.Ş., Özacar, M., *J. Hazard. Mater.* 157 (2008) 277.
3. Maheswari P., Venilamani N., Madhavakrishnan S., Syed Shabudden P.S., Venckatesh R., Pattabhi S., *Electronic J. Chem.* 5 (2008) 233
4. Karthikeyan, T.S., Rajgopal, S., Miranda, L.R., *J. Hazard. Mater.* 124 (2005) 192.
5. Kanan, N., Rengasamy G., *Water Air and Soil Pollut.* 163 (2005) 185.
6. Amuda, O.S., Giwa, A.A., Bello, I.A., *Biochemical Eng. J.* 36 (2007) 174.
7. Shukla, S.R., Roshan, S.P., *Separ. Purif. Technol.* 43 (2005) 1.
8. Doula, M., Ioannou, A., Dimirkou, A., *Adsorption.* 6 (2000) 325.
9. Xueyuan, Gu., Evans Les, J., *J. Colloid Interface Sci.* 307 (2007) 317.
10. Panday, K.K., Prasad, G., Singh, V.N., *Wat. Res.* 19 (1985) 869.
11. Verma D., Gope P.C., Maheshwari M.K., Sharma R.K., *J. Mater. Environ. Sci.* 3 (6) (2012) 1079.
12. Jha, V.K., Matsuda, M., Miyake, M., *J. Hazard. Mater.* 160 (2008) 148.
13. Biškup, B., Suboti, B., *Separ. Purif. Technol.* 37 (2004) 17.
14. Srivastava, S.K., Tyagi, R., Pant, N., *Wat. Res.* 23 (1989) 1161.
15. Vengris, T., Binkiene, R., Sveikauskaite, A., *Appl. Clay Sci.* 18 (2001) 183.
16. Abia, A.A., Horsfall, J.R., Didi, O., *Bioresource Technol.* 90 (2003) 345.
17. Zheng, W., Li X-m., Wang F., Yang Q., Deng P., Zeng G-m., *J. Hazard. Mater.* 157 (2008) 490.
18. Aydin, H., Bulut, Y., Yerlikaya, C., *J. Environ. Manage.* 87 (2008) 37.
19. Ofomaja, A.E., Naidoo, E.B., Modise, S.J., *J. Hazard. Mater.* 168 (2009) 909.
20. Lu, S., Gibb, S.W., *Bioresour Technol.* 99 (2008) 1509.
21. Djeribi, R., Hamdaoui, O., *Desalination* 225 (2008) 95.
22. Vogel A.I. A Textbook of Quantitative Inorganic Analysis (ELBS, London), (1984) 435.
23. Saha, P., Sanyal, S.K., *Desalination* 259 (2010) 131.
24. Rhoades J.D., Cation exchange capacity, in: *Methods of Soil Analysis Part 2. Chemical and Microbiological Properties*, second ed., American Society of Agronomy/Soil Science Society of America, Madison, WI, USA, (1982).
25. Mondal, M.K., *J. Environ. Manage.* 90 (2009) 3266.
26. Sudha, R., Kalpana, K., Rajachandrasekar, T., Arivoli S., *Electronic J. Chem.* 4(2007) 238.
27. Larous, S., Meniai, A.H., Lehocine, M.B., *Desalination* 185 (2005) 483.
28. Nasuha, N., Hameed, B.H., Azam, T., Din, M., *J. Hazard. Mater.* 175 (2010) 126.
29. Crini, G., Peindy, H.N., Gimbert, F., Robert, C., *Sep. Purif. Technol.* 53 (2007) 97.
30. Akar, S.T., Ozcan, A.S., Akar, T., Ozcan A., Kaynak, Z., *Desalination* 249 (2009) 757.
31. Ghazy, S.E., Ragab, A.H., *Indian J. Chem. Technol.* 14 (2007) 507.
32. Hanafiah, M.A.K., Zakaria, H., Wan Ngah, W.S., *Water Air and Soil Pollut.* 201 (2009) 43.
33. Anoop, K.K., Anirudhan, T.S., *Water SA.* 29 (2003) 147.
34. Elliot, H.A., Huang, C.P., *Water Res.* 15 (1981) 849.
35. Rengaraj, S., Kim, Y., Joo, C.K., Yi, J., *J. Colloid Interface Sci.* 273 (2004) 14.
36. Senthilkumar, P., Ramalingam, S., Sathyaselvabala, V., Dinesh Kirupha, S., Sivanesan, S., *Desalination* 266 (2011) 63.
37. Periasamy, K., Namasivayam, C., *Chemosphere* 32 (1996) 769.
38. Taker, M., Imamoglu, M., Saltabas, O., *Turk. J. Chem.* 23 (1999) 185.
39. Helen Kalavathy, M., Karthikeyan, T., Rajagopal, S., Miranda, L.R., *J. Colloid Interface Sci.* 292 (2005) 354.
40. Langmuir, I., *J Am Chem Soc.* 40 (1918) 1361.
41. Anirudhan, T.S., Radhakrishnan, P.G., *J. Chem. Thermodynamics.* 40 (2008) 702.
42. Chen, Z., Ma, W., Han, M., *J. Hazard. Mater.* 155 (2008) 327.
43. Freundlich, H.M.F., *J. Phys. Chem.* 57 (1906) 385.

44. Dubinin, M.M., Zaverina, E.D., Radushkevich, L.V., *J. Phy. Chem.* 21 (1947) 1351.
45. Kundu, S., Gupta, A.K., *Chem. Eng. J.* 122 (2006) 93.
46. Brunauer, S., Emmett, P.H., Teller, E., *J. Am. Chem. Soc.* 60 (1938) 309.
47. Slejko, F., Adsorption technology: a step by step approach to process, Eva Appl. Marcel Dekker, New York, (1985).
48. Ho, Y.S., Wase, D., Forster, C.F., *Water SA.* 22 (1996) 219.
49. Ho, Y.S., Mckay, G., *Water Air Soil Pollut.* 158 (2004) 77.
50. Kiran, I., Akar, T., Tunali, S., *Pro. Biochem.* 40 (2005) 3550.
51. Lale, M., Temocin, Z., Bag, H., *Fresenius Environ. Bullet.* 10 (2005) 736.
52. Salehi, P., Asghari, B., Mohammadi, F., *J. Iranian Chem. Soc.* 5 (2008) 80.
53. Ferro-Garcia, M.A., Rivera-Utrilla, J., Rodriguez-Gordillo, J., Bautista-Toledo, I., *Carbon* 26 (1998) 363.
54. Guzel, F., Yakut, H., Topal, G., *J. Hazard. Mater.* 153 (2008) 1275.
55. Sengorur, B., Ogleni, O., Ogleni, N., *Fresenius Environ. Bullet.* 15 (2006) 182.
56. Argun, M.E., Dursun, S., Ozdemir, C., Karatas, M., *J. Hazard. Mater.* 141 (2007) 77.
57. Aman, T., Kazi, A.A., Sabri, M.U., Bano, Q., *Colloid Surf. B, Biointerf.* 63 (2008) 116.
58. Badmus, M.A.O., Audu, T.O.K., Anyata, B.U., *Korean J. Chem. Eng.* 24 (2006) 246.
59. Ghazy, S.E., Ragab, A.H., *Indian J. Chem. Technol.* 14 (2007) 507.
60. Chen, J.P., Chen, W.R., Hsu, R.C., *J. Ferment. Bioeng.* 81 (1996) 458.
61. Muraleedharan, T.R., Ryengar, L., Venkobacnar, C., *Appl. Environ. Microbiol.* 61 (1995) 3507.
62. Lagergren, S., About the theory of so-called adsorption of soluble substances, der Sogenanntenadsorption geloster stoffe Kungliga Svenska Vetenska psalka de Miens Handlingar, 24, 1-39 (1898).
63. Ho, Y.S., Mckay, G., *Wat. Res.* 34 (2000) 735.
64. Weber, W.J., Morris, J.C., *J. Saint. Eng. Div. Am. Soc. Civ. Eng.* 89 (1963) 31.
65. Ho, Y.S., Mckay, G., *Adsorpt. Sci. Technol.* 20 (2002) 797.
66. Mckay, G., Otterburn, M.S., Sweeney, A.G., *Water Res.* 15 (1981) 327.
67. Sari, A., Citak, D., Tuzen, M., *Chem. Eng. J.* 162 (2010) 521.
68. Mckay, G., Blair, H.S., Finton, A., Sorption of metal ions by chitosan, in: Immobilization of ions by Biosorption, Eddles H, Hunt S, (Eds.) Ellis Herwood, Chichester, UK, (1986).
69. Sujana, M.G., Pradhan, H.K., Anand, S., *J. Hazard. Mater.* 161 (2009) 120.
70. Horsfall, M., Spiff, A.I., *Electronic. J. Biotechnol.* 8 (2005) 162.
71. Lu, H., Luan, M.T., Zhang, J.L., *EJGE.* 14 (2009) 1.
72. Osipow, L., Surface Chemistry: Theory and Industrial Applications, Krieger, New York, (1972).

(2013) www.jmaterenvironsci.com